A Biphasic Transversely Isotropic Poroviscoelastic Model for the Unconfined Compression of Hydrated Soft Tissue

H. Hatami-Marbini[1]
Department of Mechanical and Industrial Engineering,
University of Illinois at Chicago,
Chicago, IL 60607
e-mail: hatami@uic.edu;
hamed.hatami@gmail.com

R. Maulik
School of Mechanical and Aerospace Engineering,
Oklahoma State University,
Stillwater, OK 74075

The unconfined compression experiments are commonly used for characterizing the mechanical behavior of hydrated soft tissues such as articular cartilage. Several analytical constitutive models have been proposed over the years to analyze the unconfined compression experimental data and subsequently estimate the material parameters. Nevertheless, new mathematical models are still required to obtain more accurate numerical estimates. The present study aims at developing a linear transversely isotropic poroviscoelastic theory by combining a viscoelastic material law with the transversely isotropic biphasic model. In particular, an integral type viscoelastic model is used to describe the intrinsic viscoelastic properties of a transversely isotropic solid matrix. The proposed constitutive theory incorporates viscoelastic contributions from both the fluid flow and the intrinsic viscoelasticity to the overall stress-relaxation behavior. Moreover, this new material model allows investigating the biomechanical properties of tissues whose extracellular matrix exhibits transverse isotropy. In the present work, a comprehensive parametric study was conducted to determine the influence of various material parameters on the stress–relaxation history. Furthermore, the efficacy of the proposed theory in representing the unconfined compression experiments was assessed by comparing its theoretical predictions with those obtained from other versions of the biphasic theory such as the isotropic, transversely isotropic, and viscoelastic models. The unconfined compression behavior of articular cartilage as well as corneal stroma was used for this purpose. It is concluded that while the proposed model is capable of accurately representing the viscoelastic behavior of any hydrated soft tissue in unconfined compression, it is particularly useful in modeling the behavior of those with a transversely isotropic skeleton.
[DOI: 10.1115/1.4032059]

1 Introduction

Over the past few decades, a large number of numerical and experimental studies have been conducted to understand the multiphase biomechanical properties of soft hydrated tissues such as articular cartilage, intervertebral disk, and cornea. The in vitro unconfined and confined compression experiments are among the most widely used methods. From a theoretic viewpoint, while different variations of the classical mixture theory have been used to numerically represent unconfined compression experimental measurements [1], the isotropic biphasic model is the most commonly used [2]. This model was first proposed in 1980 for the behavior of the articular cartilage by utilizing the mixture theory formulation of Green and Naghdi [3] and Bowen [4]. The biphasic mixture theory assumes that the tissue is composed of a solid phase with linear elastic behavior and an incompressible viscous fluid phase. These assumptions result in a system of coupled differential equations which can be solved analytically to determine the mechanical response of the tissue. It is well-known that the biphasic theory ascribes the compression creep and stress–relaxation behavior of a hydrated tissue to the flow-dependent viscoelasticity, which is caused by the fluid flow within the porous solid skeleton. Despite close agreement between the model predictions and experimental measurements in confined compression, there is substantial difference between the two when the tissue is tested in unconfined compression [2,5–7]. Incorporating intrinsic viscoelasticity, anisotropy, inhomogeneity, and/or nonlinear bimodular behavior of a soft tissue are among possible ways that have been proposed to enhance the agreement between the biphasic theory predictions and experimental data [6,8–17].

The primary ingredients of the extracellular matrix of the hydrate soft tissue are collagen fibrils and a proteoglycan matrix, both of which are known to display viscoelastic behavior [18–20]. Therefore, in addition to the frictional interaction between the solid and fluid phase, the intrinsic viscoelasticity of the tissue can dissipate energy. In a series of articles, Mak et al. [8,9] proposed a biphasic poroviscoelastic model which accounts for the intrinsic viscoelasticity of the solid phase, i.e., flow-independent viscoelasticity. Cohen et al. [12] proposed a linear transversely isotropic biphasic model based on the idea that the resistance of the solid matrix against radial expansion in unconfined compression produces large tensile strain in transverse direction (transversely isotropic behavior). DiSilvestro et al. investigated the ability of the linear biphasic theory, the linear poroviscoelastic model, and the linear transversely isotropic model to simulate simultaneously the lateral displacement and the stress-relaxation response of articular cartilage in unconfined compression. They concluded that only the linear biphasic poroviscoelastic model could curve-fit successfully the experimental results [7]. Soulhat et al. [13] proposed a fibril-network reinforced model in which collagen fibrils can only resist tensile stresses. The parameters of this composite model for unconfined compression are directly related to those of the transversely isotropic biphasic model [12]. Soltz and Ateshian [14] combined the conewise linear elasticity (CLE) model of

[1]Corresponding author.
Manuscript received August 14, 2015; final manuscript received November 8, 2015; published online January 29, 2016. Assoc. Editor: Kristen Billiar.

Curnier et al. [21] and the linear isotropic biphasic model together in order to account for the tension–compression nonlinearity of solid phase. This model was later extended such that it could capture the intrinsic viscoelasticity of the solid matrix [17]. In addition to these studies, there have been many other theoretical models with the purpose of explaining the mechanical behavior of articular cartilage and similar hydrated tissue [22–27]. Nevertheless, the field lacks a linear transversely isotropic poroviscoelastic model. This model is especially important when the particular microstructure of the tissue, e.g., corneal stroma, necessitates the use of a transversely isotropic material model.

The cornea is a transparent soft tissue which refracts incoming light rays and acts as a protective shield for the eye. The biomechanical properties of cornea have been the subject of much research [28–36]. These studies have clearly shown that the cornea is a rate-dependent, anisotropic, and viscoelastic biomaterial. The corneal extracellular matrix, stroma, forms 90% of the thickness and dominates its biomechanical properties. In stroma, flat sheets of collagen fibrils (called lamellae) lie parallel to the surface while being embedded in a hydrated matrix formed by proteoglycans and interstitial fluid. Within each lamella, the collagen fibrils are parallel to each other and are packed in a quasi-regular hexagonal lattice structure [35]. Because of this particular arrangement of the lamella, the corneal stromal microstructure is transversely isotropic with the axis of symmetry normal to its surface. In other words, the properties are the same in all directions within the plane of material isotropy (tangent plane) but are different in the direction normal to this plane. In a recent study, Hatami-Marbini and Etebu [37] conducted unconfined compression experiments on corneal stroma and showed that a linear transversely isotropic biphasic model can be used to analyze experimental measurements and obtain a relatively accurate estimate for in-plane and out-of-plane corneal material properties as a function of thickness. Since this model was not able to "fully" curve-fit the experimental stress-relaxation history, they suggested that an improved representation of corneal unconfined compression experiments might be possible by accounting for the intrinsic viscoelasticity of the tissue constituents [38]. The short-term and primary objective of the present work is to take the first step for testing this hypothesis, i.e., proposing a linear transversely isotropic poroviscoelastic model in order to incorporate the intrinsic flow-independent viscoelasticity. The long-term objectives are to describe the mechanical behavior of cornea in unconfined compression using this theoretic model and determine its rate-dependent material parameters. To this end, the present study develops a linear transversely isotropic poroviscoelastic model, investigates quantitatively the effects of flow-independent and flow-dependent viscoelasticity on unconfined compression stress relaxation history, and compares the predictions of the proposed model with those of the currently available models such as the linear transversely isotropic, viscoelastic, and conewise viscoelastic theory.

2 Model Formulation

The present theory is an extension of previous models proposed by Cohen et al. [12] and Mak et al. [9], i.e., it incorporates the linear viscoelasticity of the solid matrix into the transversely isotropic biphasic theory. Although this model may be used to represent the mechanical response of any hydrated soft tissue, it is primarily intended to improve the accuracy of theoretic predictions of corneal stromal behavior in unconfined compression.

In biphasic mixture theory, the total stress is written as

$$\sigma = -p\mathbf{I} + \sigma^{\mathrm{vs}} \tag{1}$$

where $\mathbf{I} = (\,1 \quad 1 \quad 1 \quad 0 \quad 0 \quad 0\,)^{\mathrm{T}}$, p is the interstitial fluid pressure, and $\sigma^{\mathrm{vs}} = (\,\sigma_{rr} \quad \sigma_{\theta\theta} \quad \sigma_{zz} \quad \sigma_{\theta z} \quad \sigma_{zr} \quad \sigma_{r\theta}\,)^{\mathrm{T}}$ is the stress vector of the viscoelastic solid matrix which is expressed by

$$\sigma^{\mathrm{vs}} = \int_{-\infty}^{t} g(t-\tau)\mathbf{S}^{\mathrm{eq}^{-1}} : d\varepsilon(\tau) \tag{2}$$

In the above equation, $\varepsilon = (\,\varepsilon_{rr} \quad \varepsilon_{\theta\theta} \quad \varepsilon_{zz} \quad 2\varepsilon_{\theta z} \quad 2\varepsilon_{zr} \quad 2\varepsilon_{r\theta}\,)^{\mathrm{T}}$ is the strain vector, $\mathbf{S}^{\mathrm{eq}}$ represents the intrinsic equilibrium compliance matrix, and $g(t)$ is the relaxation function defined as

$$g(t) = 1 + \int_{-\infty}^{t} \frac{H(\tau)}{\tau} e^{-t/\tau} d\tau \tag{3}$$

where $H(\tau)$ is the relaxation spectrum commonly denoted by the box spectrum [39]

$$H(\tau) = \begin{cases} c & \tau_1 \le \tau \le \tau_2 \\ 0 & \text{otherwise} \end{cases} \tag{4}$$

It is noted that c is a dimensionless constant and τ_1 and τ_2 define the period of time during which relaxation occurs. For the box spectrum, the reduced relaxation function simplifies to $g(t) = 1 + c(E(-t/\tau_1) - E(-t/\tau_2))$, where $E(x) = -\int_{-x}^{\infty} e^{-t}/t\ dt$ and $g(0) = 1 + c\ln(\tau_2/\tau_1)$, and $g(\infty) = 1$.

In (r, θ, z) cylindrical coordinates and when the $r-\theta$ plane is the plane of isotropy, the intrinsic equilibrium compliance matrix of a transversely isotropic material is given by

$$\mathbf{S}^{\mathrm{eq}} = \begin{pmatrix} s_{rr} & s_{r\theta} & s_{rz} & 0 & 0 & 0 \\ s_{r\theta} & s_{rr} & s_{rz} & 0 & 0 & 0 \\ s_{rz} & s_{rz} & s_{zz} & 0 & 0 & 0 \\ 0 & 0 & 0 & s_{44} & 0 & 0 \\ 0 & 0 & 0 & 0 & s_{44} & 0 \\ 0 & 0 & 0 & 0 & 0 & s_{66} \end{pmatrix} \tag{5}$$

where $s_{rr} = 1/E_{rr}$, $s_{r\theta} = -\nu_{r\theta}/E_{rr}$, $s_{rz} = -\nu_{rz}/E_{rr}$, $s_{zz} = 1/E_{zz}$, $s_{44} = 1/\,G_{\theta z}$, and $s_{66} = 2(s_{rr} - s_{r\theta})$. The independent elastic constants are the respective in-plane and out-of-plane elastic moduli E_{rr} and E_{zz}, the respective in-plane and out-of plane Poisson's ratios $\nu_{r\theta}$ and ν_{rz}, and the out-of-plane shear modulus $G_{\theta z}$. Darcy's law gives the constitutive equation describing the relation between the fluid flux and the interstitial fluid pressure

$$\phi^f(\mathbf{v}^f - \mathbf{v}^s) = -\kappa\nabla p \tag{6}$$

where ϕ^f is the fluid phase volume fraction, $\mathbf{v}^f$ is the fluid phase velocity, $\mathbf{v}^s$ is the solid phase velocity, and κ is the permeability coefficient. The boundary conditions (see Fig. 1) for a circular button of radius r_0 in a ramp–relaxation unconfined compression experiment with frictionless conditions at the loading platens are

$$\begin{aligned} \sigma_{rr}|_{r=r_0} = p|_{r=r_0} = u_r|_{r=0} = 0 \\ \varepsilon_{zz} = \dot{\varepsilon} t H(t) - \dot{\varepsilon}(t-t_0)H(t-t_0) \end{aligned} \tag{7}$$

where $H(t)$ is Heaviside function, $\dot{\varepsilon}$ is the applied constant strain rate, and t_0 is the ramp time. Let $\mathbf{u} = (\,u_r \ u_\theta \ u_z\,)^{\mathrm{T}}$ denotes the displacement vector where $u_r = u_r(r,t)$, $u_\theta = 0$, and $u_z = z\ \varepsilon_{zz}$ are the radial, tangential, and transverse displacement components, respectively [12,40]. Using the above equations and after some manipulation, the governing equations of the biphasic model [40] simplify to a set of coupled differential equations for radial displacement and pressure in time domain. Applying Laplace transform to these equations, we obtain

$$\begin{aligned} \frac{\partial^2 \bar{u}_r}{\partial r^2} + \frac{\partial \bar{u}_r}{r\partial r} - \left(\frac{1}{r^2} + f\right)\bar{u}_r = \frac{f}{2} r \bar{\varepsilon}_{zz} \\ \frac{\partial \bar{p}}{\partial r} = \frac{s}{\kappa}\left(\bar{u}_r + \frac{\bar{r}}{2}\bar{\varepsilon}_{zz}\right) \end{aligned} \tag{8}$$

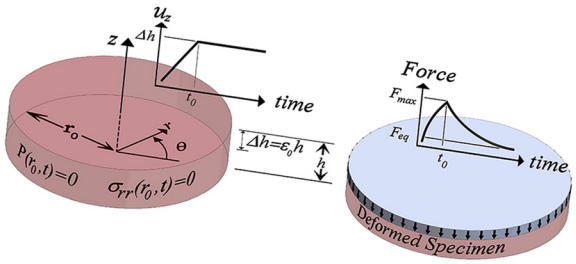

Fig. 1 A schematic plot of the unconfined compression test. A cylindrical button of tissue with radius r_0 is subjected to ramp displacement of Δh over ramp time of t_0. The measured reaction force shows a stress-relaxation behavior which reaches a peak value F_{max} and relaxes to equilibrium force F_{eq}.

where κ is the permeability coefficient, overbar represents Laplace transformed quantities, s is the Laplace transform variable, and

$$f = \frac{r_0^2 s}{\hat{E}\ \kappa\ (1 + c\ln((1+s\tau_2)/(1+s\tau_1))}$$
$$\hat{E} = 2(s_{rr}s_{zz} - s_{rz}^2)\xi,\ \xi = (s_{zz}(s_{rr}+s_{r\theta}) - 2s_{rz}^2)^{-1} \quad (9)$$

The solution of equations (8) gives

$$\bar{u}_r = \bar{\varepsilon}_{zz}\frac{(2s_{rz}+s_{zz})(s_{rr}-s_{r\theta})\xi I_1[\sqrt{f}r/r_0]}{\hat{E}\sqrt{f}I_0[\sqrt{f}] - 2I_1[\sqrt{f}]} - \frac{\bar{\varepsilon}_{zz}r}{2r_0}$$
$$\bar{p} = \hat{E}\xi\frac{(2s_{rz}+s_{zz})}{2}\left(1 + c\ln\left(\frac{1+s\tau_2}{1+s\tau_1}\right)\right)$$
$$\times\sqrt{f}\frac{I_0[\sqrt{f}r/r_0] - I_0[\sqrt{f}]}{\hat{E}\sqrt{f}I_0[\sqrt{f}] - 2I_1[\sqrt{f}]}\bar{\varepsilon}_{zz} \quad (10)$$

where $\bar{\varepsilon}_{zz} = (1 - e^{-st_0})\varepsilon_0/s^2$, $\varepsilon_0 = \dot{\varepsilon}t_0$, and $I_0[\circ]$ and $I_1[\circ]$ are the first- and second-order modified Bessel functions, respectively.

It is noted that although the present study only discusses ramp–relaxation unconfined compression experiments (7), the solution for other loading conditions is readily available by replacing their corresponding $\bar{\varepsilon}$ in Eq. (10). For instance, replacing $\bar{\varepsilon}_{zz}$ with ε_0/s gives the displacement and pressure for a step compressive strain of magnitude ε_0. The average axial stress $\bar{\sigma}$ (defined as total axial force per unit area) in Laplace domain is obtained from

$$\bar{\sigma} = \frac{1}{\pi r_0^2}\int_0^{r_0}(-\bar{p} + \bar{\sigma}_{zz})2\pi r dr \quad (11)$$

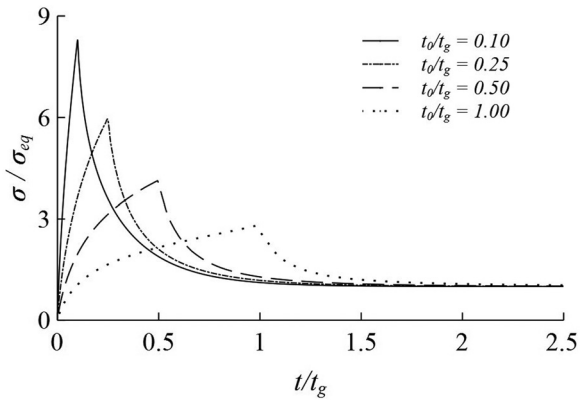

Fig. 2 The effect of the parameter t_0/t_g on the unconfined compression stress-relaxation behavior

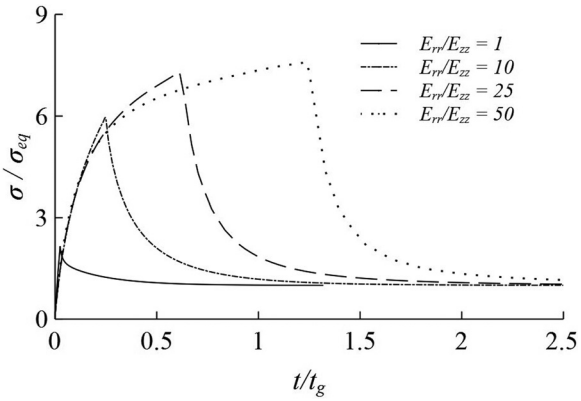

Fig. 3 The effect of the parameter E_{rr}/E_{zz} on the unconfined compression stress-relaxation behavior

and a numerical Laplace Inversion algorithm [41] is used to invert the above solution (Eqs. (10) and (11)) from Laplace domain to time domain.

3 Results

It is first noted that the model proposed here reduces to the linear transversely isotropic biphasic theory by setting $c = 0$ and to linear isotropic biphasic model by letting $c = 0$, $E_{rr} = E_{zz} = E$, and $\nu_{r\theta} = \nu_{rz} = \nu$, and $s_{44} = s_{66} = E/2(1+\nu)$. The linear transversely isotropic poroviscoelastic model has nine material constants, i.e., E_{rr}, E_{zz}, $\nu_{r\theta}$, ν_{rz}, $G_{\theta z}$, κ, c, τ_1, and τ_2. The shear modulus does not appear in predicting the behavior of cylindrical specimens in unconfined compression (Eqs. (10) and (11)), and shear tests are required for estimating $G_{\theta z}$ [42]. The effects of the remaining model parameters are discussed in the following.

In Figs. 2–7, time is normalized with respect to gel diffusion time $t_g = [r_0^2/(\hat{E}\ \kappa)]$ and stress is normalized with respect to the equilibrium stress σ_{eq}. The influence of the parameter t_0/t_g on the normalized stress–relaxation behavior is shown in Fig. 2. It is seen that increasing the ratio of ramp time t_0 and diffusion time t_g results in a smaller peak stress and subsequently shorter relaxation period. The ramping time t_0 (which is proportional to the applied strain rate when the total strain is constant), the permeability coefficient κ, and the sample radius r_0 only affect the t_0/t_g parameter. Therefore, for experiments with constant strain rate, the amount of flow-dependent relaxation is inversely proportional to the permeability coefficient κ, and directly proportional to the square of sample radius r_0.The gel diffusion time also depends on the first component of the equilibrium stiffness matrix $\hat{E}$ which is a function of E_{rr}, E_{zz}, $\nu_{r\theta}$, and ν_{rz} (see Eq. (9)). Therefore, in addition to

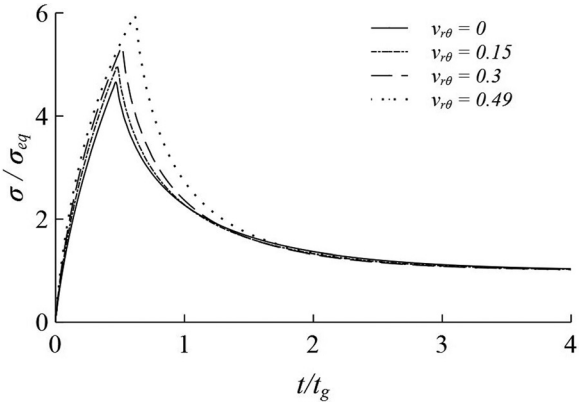

Fig. 4 The effect of the Poisson's ratio $\nu_{r\theta}$ on the unconfined compression stress-relaxation behavior

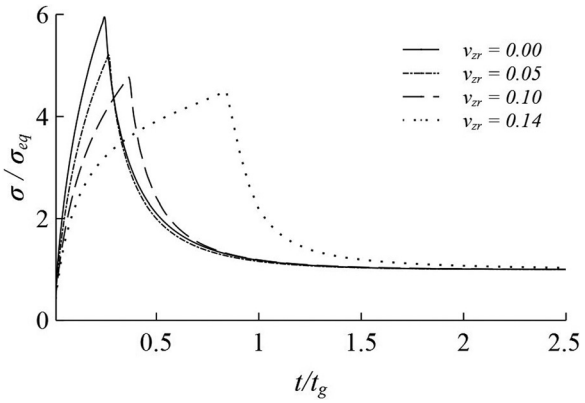

Fig. 5 The effect of the Poisson's ratio ν_{zr} on the unconfined compression stress-relaxation behavior

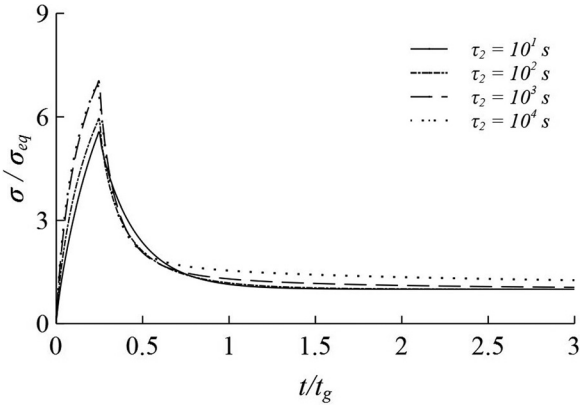

Fig. 7 The effect of the parameter τ_2 on the unconfined compression stress-relaxation behavior

its influence on the gel diffusion time, $\hat{E}$ affects the mechanical response of the solid skeleton. The influence of equilibrium stiffness matrix components is studied in Figs. 3–5. The normalized reaction force for different values of E_{rr}/E_{zz} is depicted in Fig. 3. With increasing the ratio of out-of-plane and in-plane equilibrium moduli, a higher peak stress is obtained. Nevertheless, because of the inverse relation between E_{rr} and t_g, the stress–relaxation behavior becomes more similar to that of the slow rate unconfined compression experiments. Figures 4 and 5 show the effect of the Poisson's ratio $\nu_{r\theta}$ and ν_{rz} on the stress–relaxation time history. It is seen that while both affect the mechanical response, the out-of-plane Poisson's ratio has a much more significant influence on the shape of the viscoelastic behavior of the specimen. This is an important observation since Poisson's ratios are often fixed prior to curve-fitting the experimental measurements [12,37].

Figures 6 and 7 show how the intrinsic viscoelasticity, characterized by c, τ_1, and τ_2, affects the stress–relaxation behavior of a linear transversely isotropic biphasic poroviscoelastic material. The parameter c determines the strength of viscoelasticity, and parameters τ_1 and τ_2 define the time range over which relaxation occurs. It is seen that with increasing c and τ_2, the flow-independent viscoelasticity becomes more pronounced and the material reaches a higher peak stress. The relaxation time constant τ_1 exhibits no significant effect when it is varied from 0.001 to 1 s and gives a similar curve as shown in Fig. 7.

4 Discussion

The primary objective of the present work was to develop a linear transversely isotropic biphasic poroviscoelastic model for the mechanical behavior of the hydrated soft tissue in unconfined compression. Previous studies have shown that the linear isotropic biphasic model [2,5] is unable to represent the unconfined compression mechanical behavior of the cornea and cartilage [12,37]. In order to improve the agreement between numerical models and experimental measurements, several theoretic models including linear isotropic poroviscoelastic biphasic models, linear transversely isotropic biphasic model, and bimodular poroviscoelastic biphasic model have been proposed [7,9,10,12,17]. Nevertheless, there is no previous work on a linear transversely isotropic biphasic poroviscoelastic model. The linear transversely isotropic biphasic model has previously been used to model the stress–relaxation of articular cartilage in unconfined compression experiments [12]. Although, compared to the linear isotropic biphasic model [5], this model was shown to provide a better numerical representation of unconfined compression experimental measurements, it did not get much attention in the cartilage literature. The microstructure of the corneal extracellular matrix is transversely isotropic and consists of collagen lamellae primarily lying parallel to the surface of the tissue [35,43]. Therefore, the mechanical behavior of corneal stroma needs to be analyzed at least with a transversely isotropic material model. Recently, Hatami-Marbini and Etebu showed that the transversely isotropic biphasic model can be used to analyze the unconfined compression experimental data and determine the material properties of the corneal stroma [37]. Nevertheless, they observed that this model was not able to fully represent the experimental stress-relaxation behavior. Collagen fibrils and the proteoglycan matrix,

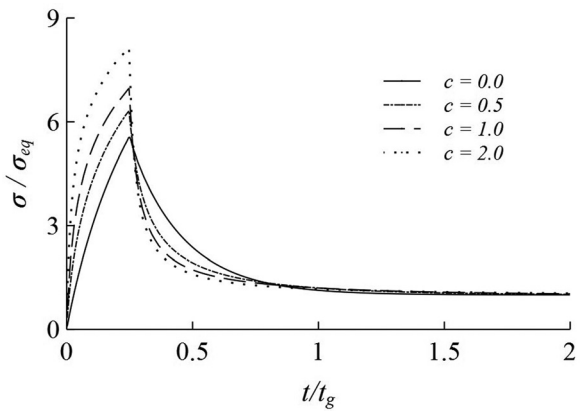

Fig. 6 The effect of the parameter *c* on the unconfined compression stress-relaxation behavior

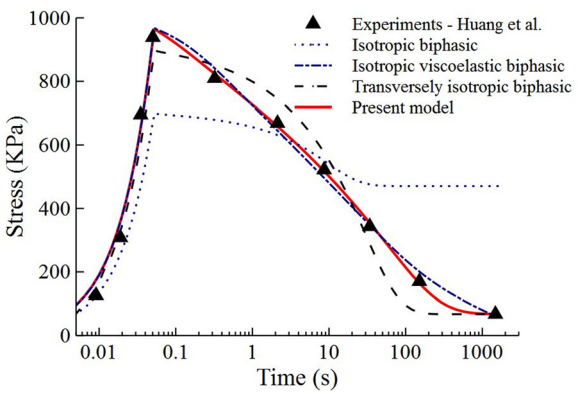

Fig. 8 The mechanical behavior of articular cartilage in a typical unconfined compression experiment (Huang et al.) and the theoretical curve-fits obtained from four different biphasic models, i.e., the linear isotropic biphasic, isotropic viscoelastic biphasic, transversely isotropic biphasic, and transversely isotropic viscoelastic (present model) theories. The time is plotted in logarithmic scale in order to highlight the capability of different models in representing the experimental measurements.

the primarily constituents of the corneal extracellular matrix, are viscoelastic [18–20]. Also, uniaxial tensile experiments on corneal strips confirmed that the tissue has viscoelastic behavior [38]. Therefore, it can be hypothesized that a linear transversely isotropic poroviscoelastic model will give a better theoretical representation of the constitutive behavior of the corneal tissue and result in a more accurate assessment of its material parameters. Accurate material constitutive models are crucial for conducting realistic numerical simulations of the complex biomechanical behavior of soft tissue; they may even lead to a way of systematically investigating the viability of therapeutic interventions by computational models. The present study focuses on developing the poroviscoelastic theory, conducting parametric study, and comparing its predictions with other available analytic models.

The poroviscoelastic model formulation includes the contributions from both the fluid flow and the intrinsic viscoelasticity to the overall stress–relaxation of the hydrated tissue under unconfined compression. The model has nine material constants: five elastic parameters, one permeability coefficient, and three viscoelastic parameters. Since unconfined compression experiments create no shear deformation, the shear modulus does not enter the formulation and needs to be determined separately [42]. In Figs. 2–7, the influence of the remaining constitutive material constants is thoroughly investigated. Here, similar relaxation function was considered for the components of the equilibrium stiffness matrix. This convenient assumption simplifies the mathematical complexities but is hard to be experimentally verified. Furthermore, although Figs. 4 and 5 show that Poisson's ratios play a significant role in the unconfined compression behavior, they are often set to fixed values, i.e., $\nu_{rz} = 0$ and $\nu_{r\theta} = 0.49$, before analyzing the experimental data. This is done because of the observation that the equilibrium load intensities in confined and unconfined compression tests are equal and the incompressibility of soft hydrated tissues [12,37]. If the Poisson's ratios are prescribed, the out-of-plane and in-plane moduli are the remaining components of the equilibrium stiffness tensor. While the flow-independent in-plane viscoelasticity of the cornea can be determined from uniaxial experiments [38], the intrinsic out-of-plane viscoelasticity includes the fluid flow and is difficult to be characterized experimentally. The transverse deformation of the corneal buttons involves compaction of negatively charged proteoglycans while the in-plane extension of the corneal strips causes relative sliding of collagen fibrils. While the latter is an energy dissipating process, the former is expected to be reversible and subsequently relatively less dissipating [8,9]. It is interesting to note that assuming $\nu_{rz} = 0$ removes the complicated dependence of equilibrium stiffness matrix on E_{rr}, E_{zz}, and $\nu_{r\theta}$ and allows developing another version of the transversely isotropic poroviscoelastic model such that intrinsic viscoelasticity only occurs in in-plane modulus E_{rr}. We leave the discussion of this version of model for a future work which will focus on curve-fitting the experimental results and determining the material parameters of cornea. Nevertheless, we discuss our preliminary results in the following and also compare the predictions of the proposed model with current material models in the literature.

Here, we consider two examples: unconfined compression experiments conducted by Huang et al. on articular cartilage [44] and the experiments preformed on corneal stroma. Huang et al. performed unconfined compression stress–relaxation experiments on cartilage cylindrical plugs of diameter 4.78 mm at $0.96/s$ strain rate. We also conducted a similar study on the cornea by testing cylindrical stromal plugs with diameter of 5 mm using an RSA-G2 machine (TA Instruments, New Castle, DE). Similar to our previous study [37], the thickness of the specimens was first obtained by applying a tare load. Then, a compressive strain of 5% with a strain rate equal to $0.1/s$ was applied. The details of unconfined compression experiments on cornea along with a discussion on corneal material constants will be presented in a future publication. In order to find the material constants and curve-fit the experimental data, a multidimensional curve-fitting was carried out using an objective function $f_{\text{obj}} = \sqrt{\Sigma_i(\sigma_{\text{mdl}}(t_i) - \sigma_{\text{exp}}(t_i))/\sigma_{\text{exp}}(t_\infty)}$, where t_∞ is the time at which equilibrium is reached, and $\sigma_{\text{mdl}}(t_i)$ and $\sigma_{\text{exp}}(t_i)$ represent the respective theoretic and experimental reaction stress at time t_i. Different optimization algorithms, such as modified particle swarm optimizer, differential evolution, and leapfrogging, were used and compared together to obtain a unique set of parameters ensuring the minimum value of objective function (results not shown).

Figure 8 shows the experimental measurements of Huang et al. (which were obtained from an image processing code) along with the theoretic fits obtained using different constitutive models, i.e., linear isotropic, transversely isotropic, isotropic viscoelastic, and transversely isotropic viscoelastic models. It is seen that the linear transversely isotropic poroviscoelastic model is able to represent the experimental response very accurately ($R^2 = 0.99$). The fit parameters are $E_{rr} = 7.9$ MPa, $E_{zz} = 1.34$ MPa, $\nu_{r\theta} = 0.49$, $\nu_{rz} = 0$, $\kappa = 7.8 \times 10^{-15}$ m^4/N s, $c = 0.13$, $\tau_1 = 0.054$ s, and $\tau_2 = 330$ s. It is noted that goodness of fit obtained here with transversely isotropic poroviscoelastic model is similar to that reported using a biphasic-CLE-QLV model [44]. It remains to be determined whether this is the case for other modes of deformation and if the present model can be used as an alternative mathematical model for describing the general behavior of articular cartilage. Nevertheless, as it was discussed earlier, because of the particular microstructure of corneal stroma, a transversely isotropic material model is very well-suited for representing its mechanical response. We have previously used a linear transversely biphasic model to obtain the material constants of the stroma. In Fig. 9, the typical behavior of the porcine corneal stroma under unconfined compression is shown. In this plot, the symbols show the total experimental reaction stress and the lines show the numerical model predictions. Similar to the articular cartilage, the proposed model resulted in a significant improvement in curve-fitting the unconfined compression experiments ($R^2 = 0.99$) with material constants $E_{rr} = 2.0$ MPa, $E_{zz} = 20$ KPa, $\nu_{r\theta} = 0.49$, $\nu_{rz} = 0$, $\kappa = 11 \times 10^{-14}$ m^4/N s, $c = 0.42$, $\tau_1 = 0.001$ s, and $\tau_2 = 22$ s. While the proposed transversely isotropic poroviscoelastic model provided a much better representation of the experiments conducted at higher strain rates, the difference between the predictions from different theories becomes less significant as loading rate reduces, which agrees with previous reports [44]. This could be because the flow-independent viscoelasticity is less important for experiments conducted at slow rate. The more complex models, such as biphasic-CLE-QLV model, behave similarly and are not able to capture the exact behavior of the samples in experiments in which the flow-dependent viscoelasticity is the dominant

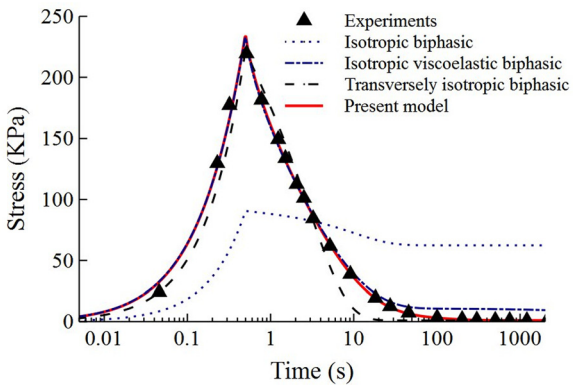

Fig. 9 The mechanical behavior of the cornea in unconfined compression and the theoretical curve-fits obtained from four different biphasic models, i.e., the linear isotropic biphasic, isotropic viscoelastic biphasic, transversely isotropic biphasic, and transversely isotropic viscoelastic (present model) theories. The time is plotted in logarithmic scale in order to highlight the capability of different models in representing the experimental measurements.

factor [44]. Finally, it is noted that besides not considering the depth-dependent properties, the present model did not consider finite deformation and/or nonlinear properties. Incorporating these features could be important but will make the constitutive model more complex and mathematically involved.

5 Conclusions

The present study combined the transversely isotropic and linear viscoelastic biphasic models in order to develop a linear transversely isotropic poroviscoelastic theory. The influence of material constants of this constitutive model on unconfined compression stress-relaxation behavior was investigated by conducting parametric studies. Furthermore, it was shown that the proposed model results in a better numerical representation of experimental measurements conducted on articular cartilage and corneal stroma, especially when they are performed at high compressive strain rates. While the present model can be used for predicting the unconfined compression behavior of any soft hydrated tissue, it is deemed to be the appropriate constitutive model for tissues (e.g., stromal cornea) with a transversely isotropic microstructure. Since the model has flow-dependent and flow-independent material constants, multiple experiments on the same sample may result in a unique and accurate estimation of these constants. In a future study, we will test the applicability of this model to characterize the viscoelastic material properties of the corneal stroma. An accurate estimate of the constitutive behavior of any soft tissue, as given by the proposed model, is vital for the success of general purpose finite element modeling and may be a significant step forward toward developing predictive numerical models for diagnosis and evaluating their biomechanical properties.

Acknowledgment

This study was supported in part by National Science Foundation (1351461).

References

[1] Hatami-Marbini, H., 2013, "Mechano-Electrochemical Mixture Theories for the Multiphase Fluid Infiltrated Poroelastic Media," *Handbook on Micromechanics and Nanomechanics*, S. Li, and X.-L. Gao Pan, eds., Stanford Publishing, Singapore, pp. 273–302.
[2] Mow, V., Kuei, S., Lai, W., and Armstrong, C., 1980, "Biphasic Creep and Stress Relaxation of Articular Cartilage in Compression: Theory and Experiments," ASME J. Biomech. Eng., **102**(1), pp. 73–84.
[3] Green, A., and Naghdi, P., 1970, "The Flow of Fluid Through an Elastic Solid," Acta Mech., **9**(3–4), pp. 329–340.
[4] Bowen, R., 1976, "Theory of Mixtures," *Continuum Physics*, A. C. Eringen, ed., Academic Press, New York.
[5] Armstrong, C., Lai, W., and Mow, V., 1984, "An Analysis of the Unconfined Compression of Articular Cartilage," ASME J. Biomech. Eng., **106**(2), pp. 165–173.
[6] Suh, J.-K., and DiSilvestro, M., 1999, "Biphasic Poroviscoelastic Behavior of Hydrated Biological Soft Tissue," ASME J. Appl. Mech., **66**(2), pp. 528–535.
[7] DiSilvestro, M. R., Zhu, Q., Wong, M., Jurvelin, J. S., and Suh, J.-K. F., 2001, "Biphasic Poroviscoelastic Simulation of the Unconfined Compression of Articular Cartilage: I–Simultaneous Prediction of Reaction Force and Lateral Displacement," ASME J. Biomech. Eng., **123**(2), pp. 191–197.
[8] Mak, A., 1986, "The Apparent Viscoelastic Behavior of Articular Cartilage: The Contributions From the Intrinsic Matrix Viscoelasticity and Interstitial Fluid Flows," ASME J. Biomech. Eng., **108**(2), pp. 123–130.
[9] Mak, A., Lai, W., and Mow, V., 1987, "Biphasic Indentation of Articular Cartilage—I. Theoretical Analysis," J. Biomech., **20**(7), pp. 703–714.
[10] Setton, L. A., Zhu, W., and Mow, V. C., 1993, "The Biphasic Poroviscoelastic Behavior of Articular Cartilage: Role of the Surface Zone in Governing the Compressive Behavior," J. Biomech., **26**(4), pp. 581–592.
[11] Schinagl, R. M., Ting, M. K., Price, J. H., and Sah, R. L., 1996, "Video Microscopy to Quantitate the Inhomogeneous Equilibrium Strain Within Articular Cartilage During Confined Compression," Ann. Biomed. Eng., **24**(4), pp. 500–512.
[12] Cohen, B., Lai, W., and Mow, V., 1998, "A Transversely Isotropic Biphasic Model for Unconfined Compression of Growth Plate and Chondroepiphysis," ASME J. Biomech. Eng., **120**(4), pp. 491–496.
[13] Soulhat, J., Buschmann, M., and Shirazi-Adl, A., 1999, "A Fibril-Network-Reinforced Biphasic Model of Cartilage in Unconfined Compression," ASME J. Biomech. Eng., **121**(3), pp. 340–347.
[14] Soltz, M. A., and Ateshian, G. A., 2000, "A Conewise Linear Elasticity Mixture Model for the Analysis of Tension-Compression Nonlinearity in Articular Cartilage," ASME J. Biomech. Eng., **122**(6), pp. 576–586.
[15] Li, L., Buschmann, M., and Shirazi-Adl, A., 2000, "A Fibril Reinforced Nonhomogeneous Poroelastic Model for Articular Cartilage: Inhomogeneous Response in Unconfined Compression," J. Biomech., **33**(12), pp. 1533–1541.
[16] Wang, C. C., Hung, C. T., and Mow, V. C., 2001, "An Analysis of the Effects of Depth-Dependent Aggregate Modulus on Articular Cartilage Stress-Relaxation Behavior in Compression," J. Biomech., **34**(1), pp. 75–84.
[17] Huang, C.-Y., Mow, V. C., and Ateshian, G. A., 2001, "The Role of Flow-Independent Viscoelasticity in the Biphasic Tensile and Compressive Responses of Articular Cartilage," ASME J. Biomech. Eng., **123**(5), pp. 410–417.
[18] Viidik, A., 1968, "A Rheological Model for Uncalcified Parallel-Fibred Collagenous Tissue," J. Biomech., **1**(1), pp. 3–11.
[19] Mow, V., Mak, A., Lai, W., Rosenberg, L., and Tang, L.-H., 1984, "Viscoelastic Properties of Proteoglycan Subunits and Aggregates in Varying Solution Concentrations," J. Biomech., **17**(5), pp. 325–338.
[20] Zhu, W., and Mow, V., 1990, "Viscometric Properties of Proteoglycan Solutions at Physiological Concentrations," *Biomechanics of Diarthrodial Joints*, V. Mow, A. Ratcliffe, and S. Woo, eds., Springer, New York, pp. 313–344.
[21] Curnier, A., He, Q.-C., and Zysset, P., 1994, "Conewise Linear Elastic Materials," J. Elasticity, **37**(1), pp. 1–38.
[22] Kwan, M. K., Lai, W. M., and Mow, V. C., 1990, "A Finite Deformation Theory for Cartilage and Other Soft Hydrated Connective Tissues—I. Equilibrium Results," J. Biomech., **23**(2), pp. 145–155.
[23] Frank, E. H., and Grodzinsky, A. J., 1987, "Cartilage Electromechanics—II. A Continuum Model of Cartilage Electrokinetics and Correlation With Experiments," J. Biomech., **20**(6), pp. 629–639.
[24] Lai, W., Hou, J., and Mow, V., 1991, "A Triphasic Theory for the Swelling and Deformation Behaviors of Articular Cartilage," ASME J. Biomech. Eng., **113**(3), pp. 245–258.
[25] Huyghe, J. M., and Janssen, J., 1997, "Quadriphasic Mechanics of Swelling Incompressible Porous Media," Int. J. Eng. Sci., **35**(8), pp. 793–802.
[26] Li, L., Buschmann, M., and Shirazi-Adl, A., 2003, "Strain-Rate Dependent Stiffness of Articular Cartilage in Unconfined Compression," ASME J. Biomech. Eng., **125**(2), pp. 161–168.
[27] Julkunen, P., Wilson, W., Jurvelin, J. S., Rieppo, J., Qu, C.-J., Lammi, M. J., and Korhonen, R. K., 2008, "Stress–Relaxation of Human Patellar Articular Cartilage in Unconfined Compression: Prediction of Mechanical Response by Tissue Composition and Structure," J. Biomech., **41**(9), pp. 1978–1986.
[28] Hatami-Marbini, H., and Etebu, E., 2013, "Hydration Dependent Biomechanical Properties of the Corneal Stroma," Exp. Eye Res., **116**, pp. 47–54.
[29] Jue, B., and Maurice, D. M., 1986, "The Mechanical Properties of the Rabbit and Human Cornea," J. Biomech., **19**(10), pp. 847–853.
[30] Hatami-Marbini, H., and Rahimi, A., 2014, "Effects of Bathing Solution on Tensile Properties of the Cornea," Exp. Eye Res., **120**, pp. 103–108.
[31] Bryant, M. R., and McDonnell, P. J., 1996, "Constitutive Laws for Biomechanical Modeling of Refractive Surgery," ASME J. Biomech. Eng., **118**(4), pp. 473–481.
[32] Nguyen, T., Jones, R., and Boyce, B., 2008, "A Nonlinear Anisotropic Viscoelastic Model for the Tensile Behavior of the Corneal Stroma," ASME J. Biomech. Eng., **130**(4), p. 041020.
[33] Hatami-Marbini, H., and Rahimi, A., 2015, "Stiffening Effects of Riboflavin/UVA Corneal Collagen Cross-Linking Is Hydration Dependent," J. Biomech., **48**(6), pp. 1052–1057.
[34] Pandolfi, A., and Holzapfel, G. A., 2008, "Three-Dimensional Modeling and Computational Analysis of the Human Cornea Considering Distributed Collagen Fibril Orientations," ASME J. Biomech. Eng., **130**(6), p. 061006.
[35] Maurice, D. M., 1984, "The Cornea and Sclera," *The Eye*, Vol. 1, Academic Press, New York, pp. 1–158.
[36] Ruberti, J. W., Sinha Roy, A., and Roberts, C. J., 2011, "Corneal Biomechanics and Biomaterials," Annu. Rev. Biomed. Eng., **13**(1), pp. 269–295.
[37] Hatami-Marbini, H., and Etebu, E., 2013, "An Experimental and Theoretical Analysis of Unconfined Compression of Corneal Stroma," J. Biomech., **46**(10), pp. 1752–1758.
[38] Hatami-Marbini, H., 2014, "Hydration Dependent Viscoelastic Tensile Behavior of Cornea," Ann. Biomed. Eng., **42**(8), pp. 1740–1748.
[39] Fung, Y., 1981, *Biomechanics: Mechanical Properties of Living Tissues*, Springer-Verlag, New York.
[40] Hatami-Marbini, H., and Etebu, E., 2012, "Rate Dependent Biomechanical Properties of Corneal Stroma in Unconfined Compression," Biorheology, **50**(3–4), pp. 133–147.
[41] De Hoog, F. R., Knight, J., and Stokes, A., 1982, "An Improved Method for Numerical Inversion of Laplace Transforms," SIAM J. Sci. Stat. Comput., **3**(3), pp. 357–366.
[42] Hatami-Marbini, H., 2014, "Viscoelastic Shear Properties of the Corneal Stroma," J. Biomech., **47**(3), pp. 723–728.
[43] Hatami-Marbini, H., and Pinsky, P. M., 2009, "On Mechanics of Connective Tissue: Assessing the Electrostatic Contribution to Corneal Stroma Elasticity," Materials Research Society Symposium, Boston, MA, Dec. 1–4, Cambridge University Press, Cambridge, UK, Vol. 1239, pp. 41–46.
[44] Huang, C.-Y., Soltz, M. A., Kopacz, M., Mow, V. C., and Ateshian, G. A., 2003, "Experimental Verification of the Roles of Intrinsic Matrix Viscoelasticity and Tension-Compression Nonlinearity in the Biphasic Response of Cartilage," ASME J. Biomech. Eng., **125**(1), pp. 84–93.